

Observation the UHE Gamma-ray emission from the J1959+2850 with LHAASO

Yanhong Yu,^{a,*} Yu Luo^b and For the LHAASO Collaboration

^a*University of Science and Technology of China,
230026 Hefei, Anhui, Peoples Republic of China*

^b*Tsung-Dao Lee Institute School of Physics and Astronomy, Shanghai Jiao Tong University,
200240 Shanghai, Peoples Republic of China*

E-mail: yuyh@ustc.edu.cn, yu_luo@sjtu.edu.cn

We report the discovery of an extended γ -ray source around the high spin-down power Fermi-LAT pulsar - 4FGL J1958+2846 with Large High-Altitude Air Shower Observatory (LHAASO), which is also resolved from previous public source LHAASO J1956+2845. The significance is 16.5 standard deviations above 25 TeV. The best-fit location is R.A. = $299.68^\circ \pm 0.05^\circ$ and decl. = $28.84^\circ \pm 0.04^\circ$, and the extension is $\sim 0.30^\circ$.

38th International Cosmic Ray Conference (ICRC2023)
26 July - 3 August, 2023
Nagoya, Japan



*Speaker

1. Introduction

The identification of accelerators, especially which can accelerate cosmic rays (CRs) to PeV (so-called PeVatrons), is a long-standing project in high-energy astrophysics. Observations of ultra-high energy (UHE, $E > 100$ TeV) gamma rays will provide key information on the origin of cosmic rays. The detection the features of UHE gamma rays produced through hadronic interactions via the pion-decay is the direct evidence of the presence of proton PeVatron in the Galaxy. However, VHE gamma rays also can produced by energetic electrons through inverse compton (IC) scattering on photon fields. The Klein-Nishina effects suppress the gamma ray emission from IC scattering in the energy range $\gtrsim 50$ TeV, and leads a an energy-dependent spectral index.

The possible candidates of Galactic sources are known to be cosmic particle accelerators: supernova remnants (SNRs), pulsar/pulsar wind nebulae (PWNe), star-forming regions, etc[1][3]. There are over 200 very high-energy (VHE, > 0.1 TeV) sources has been detected in our Galaxy. The types of most of these sources have not been identified and the spectrum can be well explained by the IC scattering on soft photon fields of energetic electrons. The detection of a significant number of gamma rays sources in TeV-PeV band is important astrophysical implications to understand the cosmic particle acceleration.

LHAASO focused on the high energy gamma ray astronomy and cosmic ray physics. Recently, LHAASO has reported 12 UHE sources with a statistical significance greater than 7σ . In this study we report our study of the region of LHAASO J1956+2845. As pointed out by cao, the possible origin of this source could be PSR J1958+2846 or SNR G66.0-0.0. The spindown luminosity of this young pulsar (age $\simeq 21.7$ kyr) is $\dot{E} \simeq 3.4 \times 10^{35}$ erg s^{-1} with a distance of 2.0 kpc. A distance of 2.3 ± 0.2 kpc was derived for the SNR G66,0-0.0 based on the red clump method. For this UHE source, the initially hot spots was revealed by Milagro at a level of 4.3σ and 4.0σ in the direction of the *Fermi* LAT source 0FL J1954.4+2838 and 0FL J1958.1+2834[10]. In the third HAWC catalog of this region, 3HWC J1954+285 is the potential TeV counterpart of LHAASO J1956+2845[9].

2. LHAASO-KM2A and WCDA experiment

LHAASO[4], a large EAS experiment located at Haizi Mountain (4410 m above sea level, in Sichuan, China), is composed of three sub-arrays, namely, KM2A, 78,000 m² water Cherenkov detector (WCDA) and wide-field air Cherenkov/fluorescence telescope array (WFCTA). Figure 1 shows the schematic of the LHAASO layout[5].

As the main array of LHAASO, KM2A consists of 5195 electromagnetic detectors (EDs) and 1188 muon detectors (MDs), with an area of 1.3 km². One half of KM2A consists of 2365 EDs and 578 MDs has been operating from 27th December 2019, three-quarter KM2A consists of 3978 EDs and 917 MDs was operated from 1th December 2020, and full KM2A has been operating from 20th July 2020. More details about the detectors are presented in [5]. WCDA mainly used for surveying transient phenomena and discovering new sources,has been built in 3 phases. The WCDA full array has been operated from March 5, 2021. More details about the detectors can be found in [5].

For KM2A, the angular resolution (denoted as ϕ_{68} , 68% containment) range from 0.5° - 0.8° at 20 TeV to 0.2° - 0.3° at 100 TeV. The energy resolution is about 24% at 20 TeV and 13% at 100 TeV. The advantage of measuring the muon component making KM2A reach a very high rejection

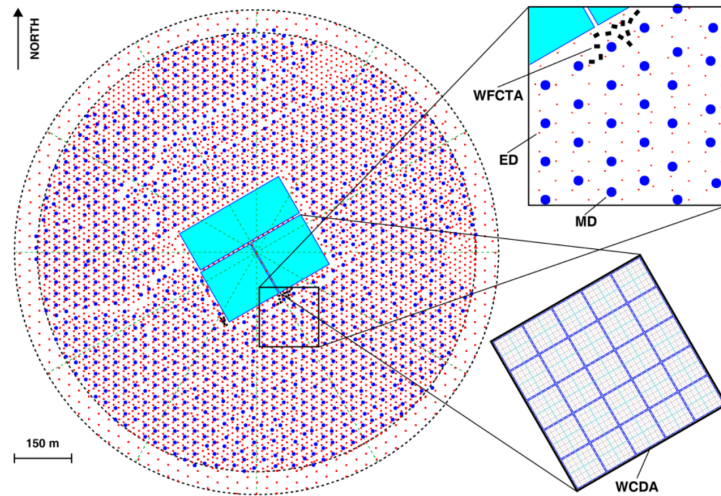


Figure 1: Schematic of the LHAASO layout.

power of cosmic ray. The fraction for γ ray ranges from 48% to 93%. The rejection power is about 10^3 at 25 TeV, and the rejection power will be better at higher energies. WCDA, consisting of three ponds with a total area of 0.08 km^2 , are sensitive to gamma-rays down to 100 GeV. The angular resolution can be reach $\delta_\phi \sim 0.2^\circ$. The sensitivity at energies $\geq 2 \text{ TeV}$ reaches the flux level of $10^{-12} \text{ erg cm}^{-2} \text{ s}^{-1}$ for a point source like the Crab Nebula in 1 year of observations.

3. Analysis method

The KM2A data sets are divided into five groups perdecade according to the reconstructed energy. WCDA used the number of triggered PMT units, referred as N_{hits} , as the shower energy estimator, and all the events are grouped in to six bins, namely $[60,100]$, $[100,200]$, $[200,300]$, $[300,500]$, $[500,800]$ and $[800,2000]$ [2]. For the data set in each group, the sky map in celestial coordinates (right ascension and declination) is divided into a grid of $0.1^\circ \times 0.1^\circ$ each pixels which are filled with the number of the detected events according to their reconstructed arrival direction (event map).

The "direct integration method" is adopted to estimate the number of cosmic-ray background events in each grid[7]. This method used events with the same direction in the horizontal coordinates but different arrival times to estimate the background. An integration of 10hr is used to estimate the detector acceptance for different directions. The number of background events in each pixel is estimated according to the detector acceptance and the event rate.

The test statistic used to evaluate the significance of the test in this work is $TS = 2\log(\lambda)$, where $\lambda = \mathcal{L}_1/\mathcal{L}_0$. \mathcal{L}_1 is the maximum likelihood value for the alternative hypothesis, and \mathcal{L}_0 is for the null hypothesis.

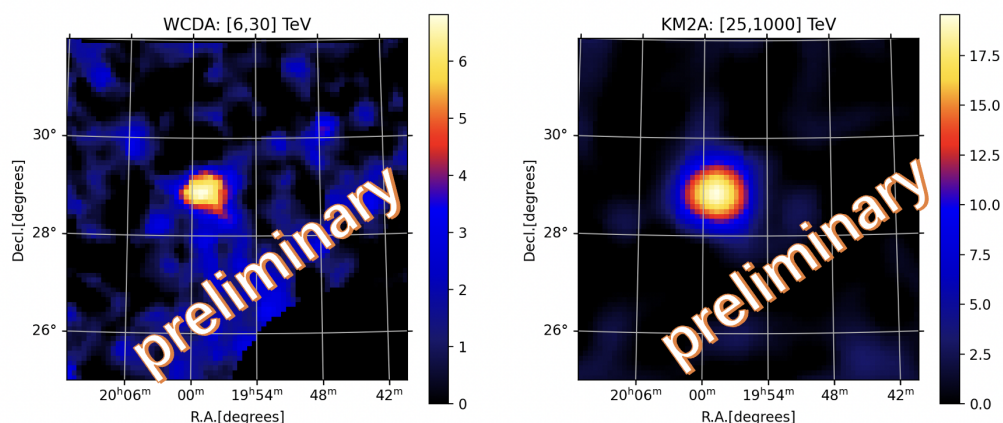


Figure 2: The significance map of LHAASO J1959+28

4. Result

The significance map of LHAASO J1959+28 are shown in Fig.2. The statistical significance of LHAASO J1959+28 is 7σ (6-30) TeV, 17σ at 25-1000 TeV.

The SED analysis and multiwavelength analysis is going on.

References

- [1] Bell A. R., 2013, APh, 43, 56. doi:10.1016/j.astropartphys.2012.05.022
- [2] F. Aharonian *et al.* [LHAASO], Performance of LHAASO-WCDA and observation of the Crab Nebula as a standard candle. doi:10.1088/1674-1137/ac041b
- [3] Aharonian F., Yang R., de Oña Wilhelmi E., 2019, NatAs, 3, 561. doi:10.1038/s41550-019-0724-0
- [4] Cao Z., 2010, ChPhC, 34, 249. doi:10.1088/1674-1137/34/2/018
- [5] He, H., For the LHAASO Collaboration. Design of the LHAASO detectors. Radiat Detect Technol Methods 2, 7 (2018). <https://doi.org/10.1007/s41605-018-0037-3>
- [6] Aharonian F., An Q., Axikegu, Bai L. X., Bai Y. X., Bao Y. W., Bastieri D., et al., 2021, ChPhC, 45, 025002. doi:10.1088/1674-1137/abd01b
- [7] Fleysher R., Fleysher L., Nemethy P., Mincer A. I., Haines T. J., 2004, ApJ, 603, 355. doi:10.1086/381384
- [8] Abeysekara A. U., Archer A., Benbow W., Bird R., Brose R., Buchovecky M., Buckley J. H., et al., 2018, ApJ, 866, 24. doi:10.3847/1538-4357/aade4e
- [9] Albert A., Alfaro R., Alvarez C., Camacho J. R. A., Arteaga-Velázquez J. C., Arunbabu K. P., Avila Rojas D., et al., 2020, ApJ, 905, 76. doi:10.3847/1538-4357/abc2d8
- [10] P. M. Saz Parkinson et al 2010 ApJ 725 571 DOI 10.1088/0004-637X/725/1/571